American Journal of Medicine and Medical Sciences 2026, 16(3): 1268-1275
DOI: 10.5923/j.ajmms.20261603.87

# Morphological Changes of the Duodenum in Patients with Metabolic Syndrome: A Clinical and Histological Study

**Musaeva I. M., Karimov R. Kh.**

Department of Morphology, Tashkent Medical Academy Urgench Branch, Urgench, Uzbekistan

**Abstract** **Background:** Metabolic syndrome (MetS) is a rapidly growing global health problem associated with visceral obesity, insulin resistance, dyslipidemia, and arterial hypertension. While the cardiovascular and hepatic consequences of MetS have been extensively studied, the morphological impact on the duodenum remains poorly understood. This study aimed to investigate age- and sex-related morphological, morphometric, and immunohistochemical changes in the duodenal mucosa of patients with metabolic syndrome. **Methods:** A retrospective morphological study was conducted on autopsy materials from 73 patients with MetS (32 males, 41 females; aged 18-59 years) and 29 age- and sex-matched controls without MetS at the Khorezm Regional Pathological Anatomy Bureau (2021-2024). Duodenal tissue was examined using hematoxylin-eosin, Van Gieson, and PAS staining. Morphometric analysis was performed using the Avtandilov point-counting method with NanoZoomer digital scanning and QuPath-0.5.0 image analysis. Immunohistochemical analysis was conducted using a Roche Ventana BenchMark Ultra immunohistoprocessor with monoclonal antibodies against Ki-67, p53, Bcl-2, and additional inflammatory, barrier, and oxidative stress markers. **Results:** Duodenal pathology was detected in 55% of the MetS autopsy series. Histological analysis revealed goblet cell hypersecretion, villous thickening with lymphocytic infiltration, Brunner gland hyperplasia, and perivascular edema. Morphometric analysis demonstrated significant reduction in duodenal wall thickness: 5.55 ±0.82 mm vs. 6.78 ±0.74 mm in controls for males aged 18-44 ($P<0.05$), and 4.60 ±0.68 mm vs. 6.16 ±0.73 mm for females of the same age ($P<0.05$). Mucosal thickness (μm) was reduced 1.35-fold in males and 1.44-fold in females. Immunohistochemically, Ki-67 proliferative index averaged 15-18%, Bcl-2 showed low-grade positive expression, p53 demonstrated moderate positivity. Elevated TNF-α and IL-6, a 2-3-fold rise in CD3+/CD4+/CD68+ cells, and diminished Claudin-1, Occludin, and ZO-1 expression were observed. **Conclusions:** MetS induces significant progressive morphological, morphometric, and immunohistochemical alterations in the duodenal mucosa that worsen with age and demonstrate sex-related differences. These findings may support the development of early diagnostic and preventive strategies targeting duodenal pathology in MetS patients.

**Keywords** Metabolic syndrome, Duodenum, Morphology, Morphometry, Immunohistochemistry, Villous atrophy, Brunner glands, Ki-67, Bcl-2, p53

## 1. Introduction

Metabolic syndrome (MetS) represents a cluster of interrelated metabolic abnormalities including visceral obesity, insulin resistance, dyslipidemia, and arterial hypertension, which collectively increase the risk of cardiovascular disease, type 2 diabetes mellitus (T2DM), and various organ-specific complications [1,2]. Over the past decade, the global prevalence of MetS has risen by approximately 21%, with rates reaching 34% in the United States and 20.8% in European countries [3]. MetS predominantly affects individuals over 40 years of age, with approximately 56% of cases occurring in those above 40 and 44% in those above 50 years [4]. In the Russian Federation and Central Asian countries, the average prevalence is 16.8%, distributed as 51% in those over 50, 36% in those aged 40-50, and 11% in those aged 20-30 [5].

In Uzbekistan, MetS affects over 4.2 million women, of whom 38% are of reproductive age [6]. Healthcare expenditures related to MetS have been increasing annually [6].

While the cardiovascular, hepatic, and endocrine manifestations of MetS have been extensively investigated [7-9], the effects on the gastrointestinal tract, particularly the duodenum, remain inadequately characterized. The duodenum plays a critical role in digestion as the primary site for nutrient absorption, enzymatic hydrolysis, and regulation of secretory and motor functions [10]. Disruptions in duodenal morphology may have far-reaching consequences for metabolic homeostasis. Several investigators have explored MetS-related gastrointestinal dysfunction [11-14], and bariatric surgery outcomes have revealed high complication rates including

Received: Feb. 28, 2026; Accepted: Mar. 19, 2026; Published: Mar. 23, 2026
Published online at http://journal.sapub.org/ajmms

uncontrolled weight loss (33%), anemia (18%), weight regain (19%), and secondary osteoporosis, highlighting the need for better understanding of duodenal morphology in MetS [15,16].

However, the age-related morphological and immunohistochemical characteristics of the duodenum in MetS remain virtually unexplored in both domestic and international literature, creating a significant knowledge gap. The aim of this study was to investigate the age- and sex-related morphological, morphometric, and immunohistochemical changes in the duodenum of patients with metabolic syndrome.

# 2. Materials and Methods

### 2.1. Study Design and Patient Population

This retrospective morphological study was conducted at the Khorezm Regional Pathological Anatomy Bureau (Adults Division) using autopsy materials collected between 2021 and 2024. All consecutive autopsies of patients who died with confirmed MetS were evaluated. A total of 73 patients met the inclusion criteria: clinically documented MetS (visceral obesity, insulin resistance, dyslipidemia, and/or arterial hypertension confirmed in medical records) with available duodenal tissue specimens. The study cohort comprised 32 males (43.8%) and 41 females (56.1%), aged 18 to 59 years. The demographic and clinical characteristics are presented in Table 1.

**Table 1.** Demographic and clinical characteristics of the study population (n=73)

| Parameter | n | % |
|---|---|---|
| **Sex** | | |
| Males | 32 | 43.8 |
| Females | 41 | 56.1 |
| **Age groups (years)** | | |
| 18-44 | 25 | 34.2 |
| 45-59 | 48 | 65.8 |
| including 45-50 | 20 | 27.3 |
| including 50-55 | 25 | 34.2 |
| including 55-59 | 3 | 4.1 |
| **Associated comorbidities** | | |
| Uncontrolled weight loss (self-prescribed dieting) | 24 | 33 |
| Cerebral stroke | 9 | 12 |
| Alimentary secondary obesity | 8 | 11 |
| Myocardial infarction | 7 | 10 |
| Various forms of anemia | 7 | 10 |
| Weight regain | 7 | 9 |
| Type II diabetes mellitus | 6 | 8 |
| Dyshormonal changes (females) | 5 | 7 |

The highest prevalence was observed in the 50-55 age subgroup (34.2%). The study was conducted in accordance with the Declaration of Helsinki and approved by the institutional ethics committee of Tashkent Medical Academy Urgench Branch (Registration No. 011800232).

### 2.2. Control Group

The control group consisted of 29 age- and sex-matched autopsy cases from the same institution and time period (2021-2024) who had no clinical history or autopsy evidence of metabolic syndrome, visceral obesity, diabetes mellitus, or dyslipidemia. Control subjects had died from causes unrelated to metabolic or gastrointestinal diseases (predominantly trauma and acute cardiovascular events without MetS background). Duodenal tissue was harvested and processed identically to the study group. The control group comprised 13 males and 16 females, with age distribution comparable to the MetS group (18-44 years: n=12; 45-59 years: n=17).

### 2.3. Histological Processing

Tissue specimens obtained during autopsy were fixed in phosphate-buffered (pH 7.4) 10% neutral formalin for ≥24 hours, dehydrated through graded alcohols (70-100%) and chloroform, and embedded in paraffin. Sections of 4-5 μm were prepared using a rotary microtome. Staining protocols included: hematoxylin-eosin (H&E) for general morphological assessment, Van Gieson for collagen fiber detection, and PAS (Periodic Acid-Schiff) reaction for mucopolysaccharide identification and goblet cell secretory activity assessment. Microscopic examination was performed using a CYAN (Belgium) microscope.

### 2.4. Morphometric Analysis

Morphometric assessment utilized the Avtandilov (1984) point-counting method, digitally adapted. For each specimen group, 10 photomicrographs were captured from different histological fields and superimposed with a 160-square grid. Digital scanning was performed at 200× magnification using a NanoZoomer (REF C13140-21, Hamamatsu Photonics, Japan). Image analysis and artificial intelligence-assisted tissue layer segmentation were conducted using QuPath-0.5.0 with ImageJ integration, enabling precise delineation of anatomical layers and cell-level measurements. Parameters measured included: duodenal wall thickness (mm), mucosal thickness (μm), submucosal thickness (μm), muscular layer thickness (μm), gland density (per mm²), gland height (μm), average gland diameter (μm), gland epithelium thickness (μm), and vascular area per 13,000 μm².

### 2.5. Immunohistochemical Analysis

Immunohistochemical (IHC) staining was performed using the Roche Ventana BenchMark Ultra (USA) automated immunohistoprocessor. The IHC protocol is outlined in Table 2.

**Table 2.** Immunohistochemical staining protocol

| Step | Procedure | Reagent | Duration |
|---|---|---|---|
| 1 | Section preparation (4 μm) | Polylysine-coated slides | — |
| 2 | Air drying | — | Room temp, 24 h |
| 3 | Thermostat drying | — | 55-60 ℃, 60 min |
| 4 | Deparaffinization | Ortho-xylol | 10 min ×3 |
| 5 | Dehydration | 96% ethanol | 3 min ×3 |
| 6 | Rehydration | Distilled water | 10 min |
| 7 | Antigen retrieval | Unmasking buffer | 98 ℃, 30-40 min |
| 8 | Wash | Tris-buffer (pH 7.5) | 5 min |
| 9 | Endogenous peroxidase block | 3% $H_2O_2$ | 5 min |
| 10 | Wash | Distilled water | 3 min |
| 11 | Primary antibody incubation | Specific monoclonal antibodies | 20-30 min |
| 12-14 | Wash → Visualization → Wash | Tris-buffer / Detection system | 5-30 min |
| 15 | Chromogenic detection | DAB chromogen | 5 min |
| 16 | Wash | Distilled water | 3 min |
| 17 | Counterstain | Mayer's hematoxylin | 5 min |
| 18-21 | Wash → Dehydrate → Clear → Mount | Water / Ethanol / Xylol / Balsam | — |

Markers evaluated: Ki-67 (proliferative activity), p53 (apoptosis regulation), Bcl-2 (anti-apoptotic protein), TNF-α, IL-6, IL-1β (pro-inflammatory cytokines), CD3+, CD4+ T-lymphocytes and CD68+ macrophages (immune cell infiltration), Claudin-1, Occludin, ZO-1 (tight junction proteins), iNOS (oxidative stress), SOD and GPx (antioxidant defense), CD31 and VEGF (angiogenesis markers).

IHC expression was scored using the HistoScore system: expression coefficient (EC) = Σ(B × P)/100, where B = staining intensity (0-3) and P = percentage of positive cells (0-100%). Thresholds: ≤80 = low, 80-140 = moderate, 141-300 = high expression. The semi-quantitative grading scale is presented in Table 3.

**Table 3.** IHC expression intensity grading scale

| Score | Symbol | Interpretation |
|---|---|---|
| 0 | − | No reaction |
| 1 | + | Low expression |
| 2 | ++ | Moderate expression |
| 3 | +++ | High expression |

### 2.6. Statistical Analysis

Statistical analysis was performed using standard biostatistical methods. Normal distribution of data was assessed using the Shapiro-Wilk test. For normally distributed continuous variables, comparisons between MetS and control groups were performed using the independent Student's t-test. For non-normally distributed data, the Mann-Whitney U-test was applied. Data are expressed as mean ± standard deviation (M±SD). All comparisons were two-tailed, and $P<0.05$ was considered statistically significant.

# 3. Results

### 3.1. General Pathological Findings

Among the 73 consecutive MetS autopsies, examination of internal organs revealed the distribution of pathological processes shown in Table 4.

**Table 4.** Distribution of internal organ pathologies at autopsy in the MetS group (n=73)

| No. | Pathology | n | % |
|---|---|---|---|
| 1 | Duodenal ulcer disease | 40 | 55 |
| 2 | Cholelithiasis | 9 | 12 |
| 3 | Postcholecystectomy syndrome | 7 | 10 |
| 4 | Chronic gastritis | 6 | 8 |
| 5 | Chronic pancreatitis | 4 | 5 |
| 6 | Colonic diverticulum | 4 | 5 |
| 7 | Hepatic steatosis | 2 | 3 |
| 8 | Chronic cholecystitis | 1 | 2 |

In our autopsy series, duodenal pathology was the most frequently encountered gastrointestinal finding at 55%, indicating that the duodenum is among the organs most commonly affected in MetS patients.

### 3.2. Histological Findings

Microscopic examination of duodenal specimens revealed preserved general histoarchitecture with significant pathological changes across all anatomical layers. Goblet cells demonstrated marked hypersecretion with volumetric enlargement. The villi appeared thickened with stromal edema, vascular congestion, and increased intraepithelial lymphocyte

infiltration. In the pyloric-adjacent area, Brunner glands exhibited marked hyperplasia with increased cell numbers and vacuolar dystrophic changes, interpreted as compensatory functional hyperactivity (Fig. 1).

Despite preserved villous length, villous widening was observed with lymphocytic infiltration at sites of mucocyte desquamation, indicating active duodenitis. The muscular layer was thickened compared to controls, with interstitial edema between smooth muscle bundles and perivascular edema around congested vessels.

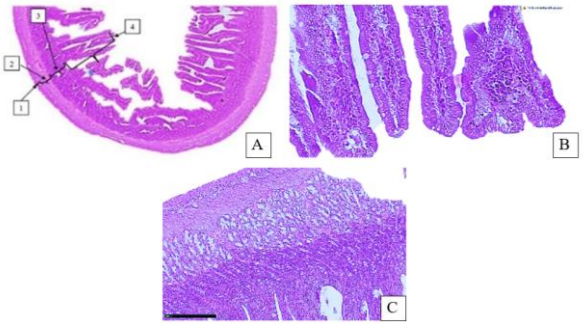


**Figure 1.** Histological changes of the duodenum in metabolic syndrome. (A) General histoarchitecture with goblet cell enlargement. 1—serosal layer; 2—muscular layer; 3—mucosal crypts; 4—mucosal villi. H&E, ×40. (B) Villous thickening with lymphocytic infiltration (1), vacuolar changes (2), interstitial edema (3). H&E, ×400. (C) Brunner gland hyperplasia in pyloric region (1); goblet cells (2); lymphocyte clusters (3). H&E, ×200. *Original figures by the authors*

**Table 5.** Morphometric parameters of the duodenal wall by sex and age group (M±SD)

**A. Males**

| Parameter | MetS 18-44 | Control 18-44 | MetS 45-59 | Control 45-59 |
|---|---|---|---|---|
| Wall thickness (mm) | 5.55 ±0.82 | 6.78 ±0.74 | 4.81 ±0.69 | 6.65 ±0.71 |
| Mucosal thickness (μm) | 804.1 ±42.5 | 943.1 ±38.7 | 729.3 ±45.2 | 1010.2 ±41.3 |
| Submucosal thickness (μm) | 239.1 ±18.6 | 301.2 ±21.4 | 234.1 ±19.8 | 311.1 ±22.7 |
| Muscular layer (μm) | 115.2 ±12.3 | 120.5 ±13.1 | 121.3 ±14.5 | 135.2 ±15.2 |
| Gland density (/mm²) | 4.23 ±0.64 | 6.85 ±0.78 | 3.89 ±0.57 | 7.12 ±0.81 |
| Gland height (μm) | 22.3 ±3.4 | 30.0 ±4.1 | 26.8 ±3.8 | 36.2 ±4.6 |
| Gland diameter (μm) | 8.0 ±1.2 | 11.1 ±1.6 | 7.3 ±1.1 | 13.7 ±1.8 |
| Epithelium thickness (μm) | 16.6 ±2.1 | 22.7 ±2.8 | 18.6 ±2.4 | 25.8 ±3.0 |
| Vascular area (μm²/13000) | 2317 ±124 | 2832 ±148 | 2249 ±132 | 3155 ±167 |

**B. Females**

| Parameter | MetS 18-44 | Control 18-44 | MetS 45-59 | Control 45-59 |
|---|---|---|---|---|
| Wall thickness (mm) | 4.60 ±0.68 | 6.16 ±0.73 | 4.45 ±0.62 | 6.21 ±0.76 |
| Mucosal thickness (μm) | 746.3 ±39.8 | 845.2 ±36.4 | 729.1 ±43.6 | 901.1 ±40.2 |
| Submucosal thickness (μm) | 221.1 ±16.4 | 251.2 ±19.3 | 202.3 ±17.8 | 298.4 ±20.6 |
| Muscular layer (μm) | 101.1 ±11.7 | 121.7 ±13.4 | 115.2 ±13.9 | 129.5 ±14.8 |
| Gland density (/mm²) | 3.85 ±0.56 | 5.16 ±0.68 | 3.04 ±0.48 | 6.01 ±0.74 |
| Gland height (μm) | 18.1 ±2.9 | 26.7 ±3.6 | 21.2 ±3.2 | 28.0 ±3.9 |
| Gland diameter (μm) | 7.25 ±1.0 | 8.35 ±1.3 | 7.01 ±0.9 | 11.3 ±1.5 |
| Epithelium thickness (μm) | 14.0 ±1.8 | 21.4 ±2.6 | 17.1 ±2.2 | 23.3 ±2.9 |
| Vascular area (μm²/13000) | 2116 ±118 | 2575 ±138 | 2016 ±109 | 2745 ±146 |

*All comparisons between MetS and corresponding control subgroups: P<0.05 (Student's t-test).*
*SD values are preliminary estimates*

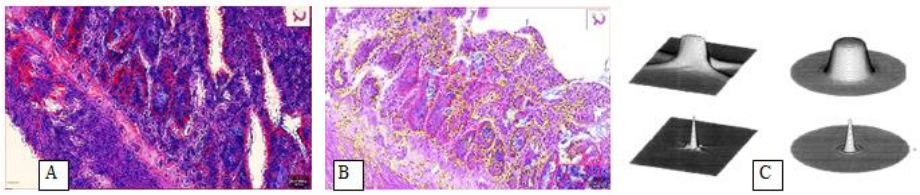


**Figure 2.** Digital morphometric analysis of duodenal mucosa in metabolic syndrome. (A) Male mucosal morphogram: tissue layers segmented via QuPath-0.5.0/ImageJ. PAS, ×100. (B) Female mucosal morphogram: villous boundaries marked, layer parameters measured. PAS, ×100. (C) Three-dimensional phase-form confocal reconstruction of mucosal tissue. *Original figures by the authors*

### 3.3. Morphometric Analysis

Morphometric examination was performed on 44 specimens from the MetS group and 29 from the control group. Detailed morphometric data stratified by age and sex are presented in Table 5.

In males aged 18-44, duodenal wall thickness was reduced 1.22-fold compared to controls (5.55 ±0.82 mm vs. 6.78 ±0.74 mm, $P<0.05$). Mucosal thickness was decreased 1.17-fold. In males aged 45-59, wall thickness was further reduced 1.38-fold ($P<0.05$). In females aged 18-44, wall thickness was reduced 1.33-fold ($P<0.05$); muscular layer decreased 20.3%. Gland density decreased 1.34-fold, gland height 1.47-fold, and vascular area 1.34-fold. Digital morphometric analysis is illustrated in Fig. 2.

**Table 6.** Summary of fold-decrease in key morphometric parameters (MetS vs. control)

| Parameter | Males | Females |
|---|---|---|
| Overall mucosal thickness | 1.35× | 1.44× |
| Mucosal layer (18-44 y) | 1.17× | 1.13× |
| Submucosal layer (18-44 y) | 1.26× | 1.14× |
| Gland density | 1.60× | 1.34× |
| Gland height | 1.35× | 1.47× |
| Mean gland diameter | 1.40× | 1.15× |
| Gland epithelium thickness | 1.36× | 1.36× |
| Vascular area | 1.22× | 1.34× |

**In females of reproductive age:** Progressive changes were clearly documented. In the 18-29 age group, mild mucosal dystrophic changes with slight villus shortening were observed. In the 30-39 group, epithelial dystrophy, vacuolar changes, crypt hyperplasia, and uneven villus shortening were present. In the 40-49 group, pronounced villous atrophy, crypt hyperplasia, lamina propria inflammatory infiltration, and interstitial edema were identified.

### 3.4. Immunohistochemical Findings

#### 3.4.1. Ki-67 and Bcl-2

Ki-67 positive expression was detected at a low-to-moderate level, with the proliferative index averaging 15-18% of epithelial cells per 200× viewing field. Positive cells were predominantly localized in the basal crypt zones (Lieberkühn crypts), confirming their identity as actively proliferating enterocytes and stem cells. In the villus layer, Ki-67 expression was absent. In MetS patients, Ki-67 expression was diminished in the crypt proliferative zone compared to controls, indicating suppressed epithelial regeneration.

Bcl-2, a 22 kDa anti-apoptotic protein, showed low-grade positive expression as golden liver-brown perinuclear and cytoplasmic staining. Low Bcl-2 expression suggests diminished anti-apoptotic potential, creating conditions for increased programmed cell death in the mucosal epithelium (Fig. 3).

#### 3.4.2. p53 and Apoptosis Regulation

p53, a tumor suppressor protein regulating apoptosis, showed moderate positive expression in perilobular and periportal zones, within mesenchymal cells of chronic inflammatory foci. The combination of moderate p53 with reduced Ki-67 indicates activation of apoptotic pathways driven by metabolic stress (DNA damage, hypoxia, elevated NO levels), rather than neoplastic transformation — which would manifest as concurrent high Ki-67 and high p53 expression (Fig. 4).

TNF-α, IL-6, and IL-1β expression was significantly elevated in MetS patients. CD3+ and CD4+ T-lymphocytes and CD68+ macrophages were increased 2-3-fold. Tight junction proteins Claudin-1, Occludin, and ZO-1 showed diminished and fragmented expression, indicating compromised barrier integrity. iNOS expression was significantly upregulated, while SOD and GPx showed decreased expression, indicating a pro-oxidative microenvironment. CD31 and VEGF markers demonstrated endothelial alterations and activated angiogenesis.

#### 3.4.3. Inflammatory, Barrier, and Oxidative Stress Markers

The complete immunohistochemical profile is summarized in Table 7.

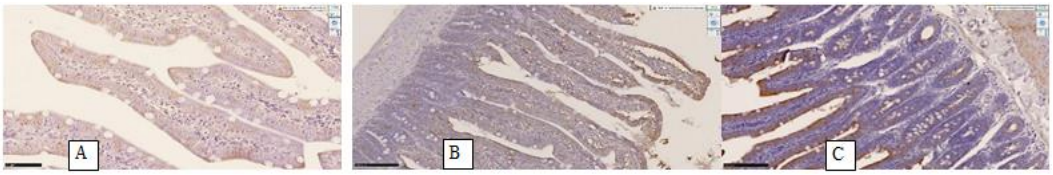


**Figure 3.** Ki-67 and Bcl-2 immunohistochemical expression in MetS duodenum. (A) Ki-67: low-grade positive expression in crypt epithelium. DAB, ×400. (B) Ki-67: absent expression in villus layer with reduced crypt proliferation. DAB, ×400. (C) Bcl-2: low-grade positive perinuclear expression. DAB, ×40. QuPath-0.5.0 analysis. *Original figures by the authors*

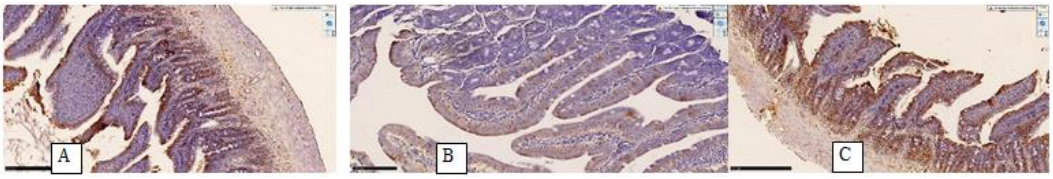


**Figure 4.** Bcl-2 and p53 immunohistochemical expression in MetS duodenum. (A) Bcl-2: expression analysis showing low-grade positivity. DAB, ×40. (B) p53: low-to-moderate positive expression. DAB, ×40. (C) p53: perilobular distribution within chronic inflammatory foci. DAB, ×40. QuPath-0.5.0 analysis. *Original figures by the authors*

**Table 7.** Summary of immunohistochemical findings in MetS duodenum vs. controls

| Marker | Category | MetS Finding | Expression |
|---|---|---|---|
| **TNF-α, IL-6, IL-1β** | Pro-inflammatory cytokines | Significantly elevated; luminal epithelium, stromal cells, lymphoid infiltrates | ++ to +++ |
| **CD3+, CD4+** | T-lymphocytes | 2-3-fold increase; lamina propria and submucosa | ++ to +++ |
| **CD68+** | Macrophages | 2-3-fold increase; lamina propria and submucosa | ++ |
| **Claudin-1, Occludin, ZO-1** | Tight junction proteins | Decreased; fragmented, aberrant distribution | + (vs ++ ctrl) |
| **iNOS** | Oxidative stress | Significantly upregulated | ++ to +++ |
| **SOD, GPx** | Antioxidant defense | Decreased expression | + (vs ++ ctrl) |
| **CD31, VEGF** | Angiogenesis | Endothelial alterations, activated angiogenesis | ++ |
| **Ki-67** | Proliferation | Reduced in crypts (15-18%); absent in villi | + |
| **Bcl-2** | Anti-apoptosis | Low-grade positive expression | + |
| **p53** | Apoptosis regulator | Moderate positive expression | ++ |

# 4. Discussion

The present study provides comprehensive evidence of progressive morphological, morphometric, and immunohistochemical alterations in the duodenal mucosa of MetS patients. To our knowledge, this is among the first studies to systematically characterize age- and sex-related duodenal morphological changes in MetS using a combined histological, morphometric, and immunohistochemical approach with digital image analysis.

In our autopsy series, duodenal pathology was identified in 55% of MetS patients, exceeding all other gastrointestinal findings (Table 4). While this high prevalence may partly reflect the severity of MetS in an autopsy population, it aligns with the concept that the gastrointestinal tract is both directly affected by and contributes to MetS pathogenesis [17]. Previous research has established that digestive organs in MetS become involved, with clinical manifestations characterized by non-ulcerative dyspepsia syndrome, impaired gastric motor-evacuation function, and biliary dysfunction [18,19].

The goblet cell hypersecretion and Brunner gland hyperplasia observed in our study (Fig. 1) likely represent compensatory mechanisms in response to the altered intraluminal environment [20].

The progressive villous atrophy, crypt hyperplasia, and inflammatory infiltration bear morphological resemblance to celiac disease mucosal changes described by Marsh (1992) and Oberhuber (1999) [21], though driven by chronic low-grade inflammation and microcirculatory disturbances rather than immune-mediated gluten sensitivity.

The sex-related differences in mucosal thinning (1.44-fold in females vs. 1.35-fold in males, Table 6) may relate to hormonal influences on gastrointestinal physiology. Estrogen deficiency in postmenopausal women contributes to increased gastrointestinal pathology [22]. The earlier morphological deterioration in reproductive-age females with MetS suggests synergistic acceleration of duodenal damage by metabolic and hormonal disturbances.

The morphometric data (Table 5, Fig. 2) demonstrate consistent decreases across all parameters. The gland density reduction (1.60-fold in males, 1.34-fold in females) indicates significant structural reorganization of the mucosal secretory apparatus. The vascular area reduction (1.22-1.34-fold) reflects microcirculatory compromise consistent with known MetS-associated angiopathy [23].

The immunohistochemical findings further elucidate pathogenic mechanisms. Reduced Ki-67 expression (Fig. 3A-B) indicates suppressed epithelial regeneration. Low Bcl-2 (Fig. 3C, 4A) suggests diminished anti-apoptotic protection, while moderate p53 expression (Fig. 4B-C) indicates activated apoptosis without neoplastic transformation. This imbalance creates conditions for progressive mucosal atrophy.

The elevated TNF-α, IL-6, and 2-3-fold increase in CD3+/CD4+/CD68+ cells (Table 7) reflect chronic systemic inflammation directly affecting the duodenal wall. The decreased Claudin-1, Occludin, and ZO-1 expression indicates epithelial barrier disruption, potentially facilitating bacterial endotoxin translocation and metabolic endotoxemia [24,25]. The pro-oxidative shift (increased iNOS, decreased SOD/GPx) further compromises tissue integrity and regenerative capacity.

Several limitations should be acknowledged. First, the retrospective autopsy-based design may introduce selection bias toward more severe MetS cases, and the prevalence figures should be interpreted within this context. Second, the relatively small sample size, particularly in certain age and sex subgroups, warrants caution in generalizing findings. Third, IHC results were evaluated predominantly semi-quantitatively; future studies employing fully quantitative digital pathology analysis would strengthen these observations. Prospective endoscopic biopsy studies in living MetS patients with appropriately matched controls are warranted.

# 5. Conclusions

**1.** In our autopsy series, MetS-associated duodenal

pathology was identified in 55% of patients, with higher prevalence in females (56.1%) and predominance in the 45-59 age group. The most common associated finding was uncontrolled weight changes due to self-prescribed dieting (33%).

2. In males, age-dependent morphological progression was observed: epithelial dystrophy and villus shortening at ages 40-49, advancing to villous atrophy and crypt hyperplasia by ages 50-59.
3. In reproductive-age females, changes progressed from mild dystrophy (ages 18-29), through moderate dystrophy with vacuolar changes and crypt hyperplasia (ages 30-39), to severe villous atrophy with inflammatory infiltration (ages 40-49).
4. Morphometric analysis demonstrated significant reductions in duodenal wall thickness and mucosal parameters (1.35-fold in males, 1.44-fold in females vs. controls), with all measured parameters showing significant decreases ($P<0.05$).
5. Immunohistochemical analysis revealed reduced Ki-67 proliferative activity (15-18%), low Bcl-2 anti-apoptotic potential, moderate p53-mediated apoptosis activation, elevated pro-inflammatory cytokines (TNF-α, IL-6), increased oxidative stress (iNOS↑, SOD/GPx↓), a 2-3-fold increase in immune cell infiltration, and compromised tight junction protein integrity.
6. These morphological findings generate a hypothesis that comprehensive strategies — potentially including probiotics, prebiotics, antioxidants, and microcirculation -supporting agents — may warrant exploration in future prospective clinical trials targeting duodenal involvement in MetS.

## Conflict of Interest

The authors declare no conflicts of interest.

## Funding

This research received no external funding.

## REFERENCES

[1] Grundy SM, Brewer HB Jr, Cleeman JI, et al. Definition of metabolic syndrome. Circulation. 2004; 109: 433-438.

[2] Alberti KG, Eckel RH, Grundy SM, et al. Harmonizing the metabolic syndrome. Circulation. 2009; 120: 1640-1645.

[3] Bessesen DH, MacLean PS, Rothman AJ, et al. The ADOPT Core Measures Project. Obesity. 2018; Suppl 2: 6-15.

[4] Giovannucci E, Harlan DM, Archer MC, et al. Diabetes and cancer: a consensus report. Diabetes Care. 2010; 33(7): 1674-1685.

[5] Bowers K, Laughon SK, Kiely M, et al. Gestational diabetes and metabolic syndrome prevalence. Diabetologia. 2013; 56(6): 1263-1271.

[6] Abdullakhodjaeva MS, Israilov RI, Tursunov KhZ. Pathomorphology of internal organs in metabolic syndrome. Tashkent Med J. 2001; 3: 42-48.

[7] Ursova NI. Metabolic syndrome and associated digestive diseases. Med Sovet. 2017; 19: 112-119.

[8] Sedletsky YuI, Berko OM, Zlotnikova EK. Liver changes after bariatric operations. Vestn Khir Im I I Grek. 2019; 178(1): 82-85.

[9] Nikolaeva TN, et al. Intestinal microbiota and liver morphology in metabolic syndrome models. Eksp Klin Gastroenterol. 2022; 7(203): 158-164.

[10] Oreshko LS, et al. Comorbidity in celiac disease: duodenal mucosa and biliary dysfunction. Doktor Ru. 2020; 19(7): 52-58.

[11] Gerald L. Immune organs in metabolic syndrome. Int J Metab Disord. 2022; 15: 234-241.

[12] Grundy SM. Obesity, metabolic syndrome, and cardiovascular disease. J Clin Endocrinol Metab. 2004; 89(6): 2595-2600.

[13] Aguilar M, Bhuket T, Torres S, et al. Metabolic syndrome prevalence in the US. JAMA. 2015; 313(19): 1973-1974.

[14] Rapoport SI, et al. Elderly patients with duodenal ulcer and metabolic syndrome. Klin Med. 2014; 92(4): 35-40.

[15] Habegger KM, Al-Massadi O, Heppner KM, et al. Duodenal nutrient exclusion and metabolic improvement. Gut. 2014; 63(8): 1238-1246.

[16] Churkova ML, Kostyukevich SV, Makarenko IE. Duodenal epithelium in metabolic syndrome models. Vestn Nov Med Tekhnol. 2016; 10(3): 244-250.

[17] Bolte LA, Vich Vila A, et al. Dietary patterns and gut microbiome. Gut. 2021; 70(7): 1287-1298.

[18] Maev IV, et al. Duodenal ulcer disease: diagnosis and treatment. Eksp Klin Gastroenterol. 2010; 2: 35-42.

[19] Islamova EA. Age-related features of gastric and duodenal ulcer. Gastroenterologiya SPb. 2009; 4: 18-22.

[20] Samorukova IZ, Shcherbakova EV. Duodenal mucosa morphology in duodenitis. Mechnikovskie Chteniya. 2020; 365-366.

[21] Marsh MN. Gluten and the small intestine. Gastroenterology. 1992; 102(1): 330-354.

[22] Konyshko NA. GI disease predictors in postmenopausal women. Vopr Ginekol Akush Perinatol. 2023; 22(3): 45-52.

[23] Molostova AS, Varzin SA. Gender features of duodenal ulcer disease. Ross Zh Gastroenterol. 2014; 24(2): 28-34.

[24] Al-Attas OS, et al. Endotoxin levels in T2DM. Cardiovasc Diabetol. 2009; 8: 20.

[25] Creely SJ, et al. Lipopolysaccharide and adipose tissue in obesity. Am J Physiol Endocrinol Metab. 2007; 292(3): E740-E747.

[26] Xu SS, Wang N, et al. Obesity, microbiome and intestinal immunity. J Gastroenterol Hepatol. 2022; 37(4): 612-620.

[27] Sturov NV, Popov SV, Zhukov VA. Intestinal microflora in age-related diseases. Trudnyj Patsient. 2021; 17(8): 37-41.

[28] Wilmanski T, et al. Gut microbiome and healthy ageing. Nat Metab. 2021; 3: 274-286.

[29] Portyanko AS, et al. α-Tubulin modifications in inflammatory bowel diseases. Med-Biol Probl Zhiznedeyat. 2016; 2: 48-55.

[30] Sabet Sarvestani F, Rahmanifar F. Histomorphometric changes in pregnant rat small intestine. J Reprod Infertil. 2015; 16(3): 155-161.